2 Experimental*

The 60-l stainless steel experimental chamber is kept at a base pressure of 10^{-10} mbar, as measured with an ionization gauge, by means of a turbomolecular pump. A rotary pump provides a 10^{-3} mbar fore vacuum. In between, a zeolite trap reduces the hydrocarbon contamination arising from the lubrication oil. Titanium sublimation further improves the vacuum of the chamber. Leaks and rest gases are checked by a quadrupole mass spectrometer (QMG 112A, Balzers). A backview LEED (VSI) is routinely used to check the quality of single-crystal surfaces and a small-spot Auger spectrometer (CLAM-2, VG) provides information on cleanness and adsorbate coverage of the samples.

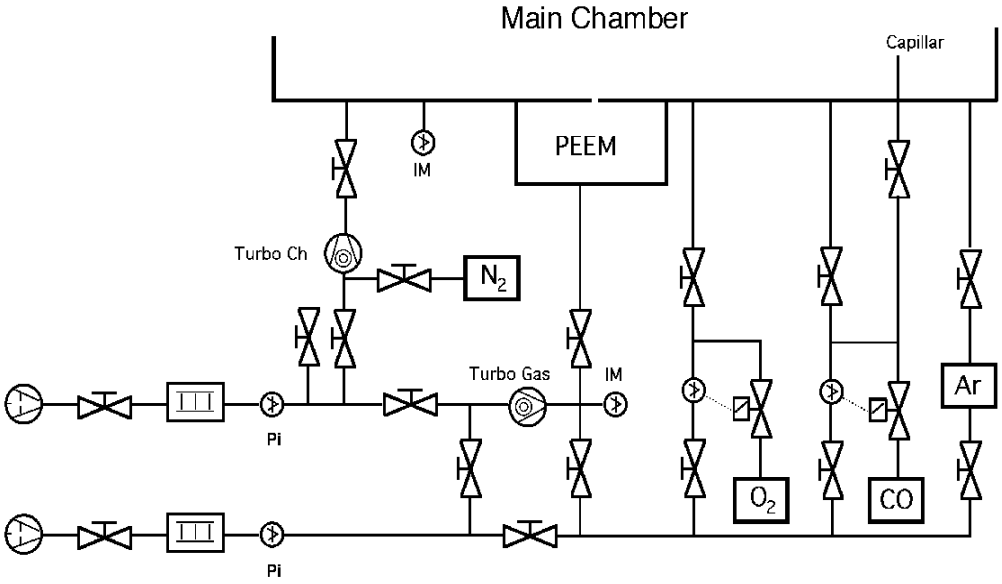

Fig. 2.1 The gas system of the experimental chamber.

Purified gases only (O_2: 999996 parts per million or, following the standard nomenclature, 5.6; CO: 99998 parts per 100'000 or 4.8; Ar: 99999 parts per 100'000 or 5) are inserted in the differentially pumped gas line, as depicted in Fig. 2.1. By means of dosing valves the range of the partial pressures is selected and (within 0.1%) stabilized via a feedback. Under reaction conditions the chamber is operated as a continuous flow reactor, by continuously pumping the system.

* Reference at page 21

Since the pumping speed largely exceeds the typical reaction rate, the partial pressure measured by QMS is proportional to the rate. The experimental techniques employed, i.e., photoemission electron microscopy (PEEM), ellipsometry for surface imaging (EMSI), and infrared thermography (IRI), are described in the following.

2.1 The Photoemission Electron Microscopy – PEEM

The method consists in forming an image of the photoelectrons emitted from a region of a metal surface irradiated by UV light with temporal and spatial resolutions of 20 ms and 0.2 µm, respectively [1]. PEEM's main characteristic is the ability to reveal the presence of adsorbates, even at submonolayer coverages. In fact, the yield of photoelectrons depends sensitively on the local, adsorbate-dependent, work function of the substrate.

The electronic images are magnified (100 to 1000 x, corresponding to a field of view of 600 to 60 µm) by a system of electrostatic lenses, amplified (typically 10^3 times) by a channelplate, projected onto a backview P20 phosphor (with a 90 to 10% decay time of 4 ms) screen, recorded by a CCD (Kappa CF8) camera and stored on SVHS video tapes. Because of pressure requirements, it is necessary to differentially pump the channelplate section below 10^{-6} mbar while performing experiments in low vacuum (10^{-3} - 10^{-4} mbar).

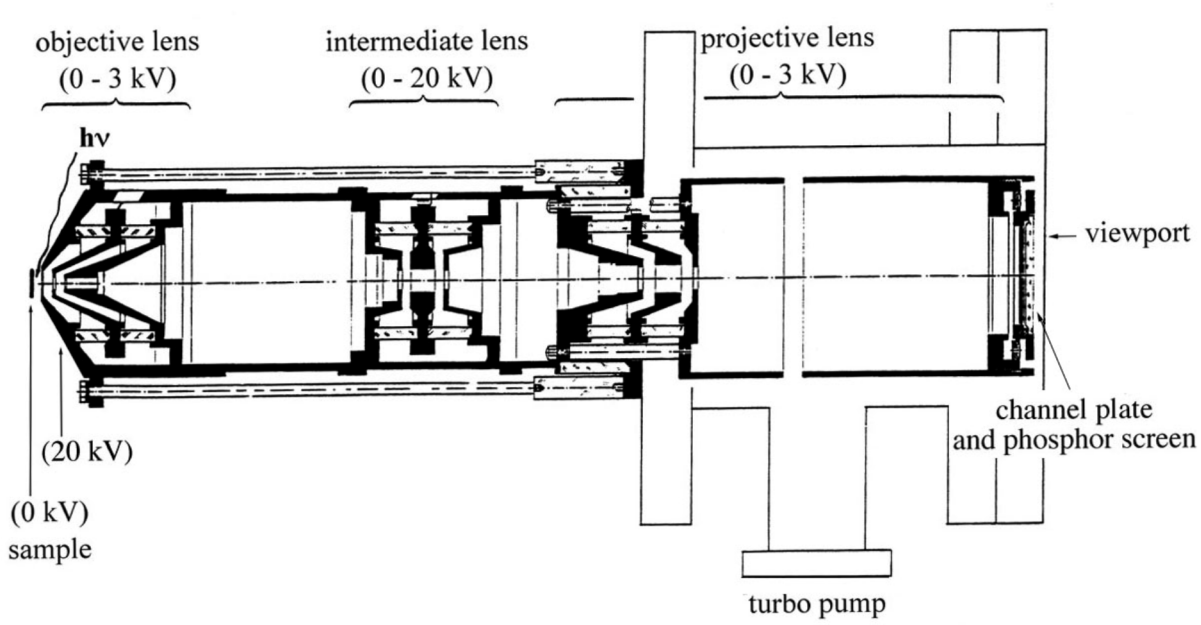

Fig. 2.2 Section view of the PEEM.

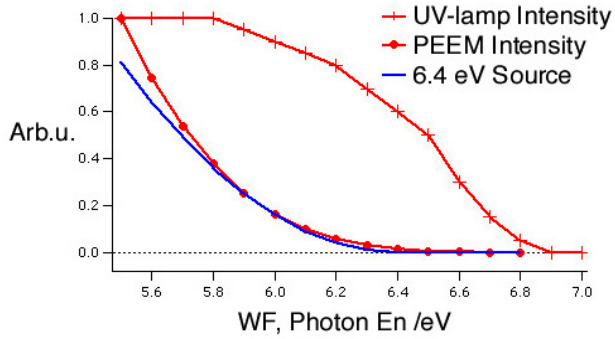

Fig. 2.3 Spectral intensity of UV lamp and calculated PEEM intensity.

A deuterium discharge lamp (200 W, Heraeus) was used as source. The photoemission yield for a spectral intensity characteristic of this source, calculated assuming a quadratic dependence of the yield (I) from the energy of the radiation (E) and the work function (WF) of the surface [2], i.e., $I \sim (E - WF)^2$ and a uniform electronic density of state close to the Fermi level (which is not the case, as shown in Sect. 1.2), is compared in Fig. 2.3 with a hypothetical 6.4 eV monochromatic source.

2.2 Ellipsometry for Surface Imaging - EMSI

A UHV-compatible version of the microscopic imaging ellipsometer [3] was developed by the Rotermund group [4] at the Fritz-Haber-Institute. EMSI makes use of the changes of the polarization upon reflection. As depicted in Fig. 2.4, monochromatic, polarized laser light is focused onto the sample. A scrambler is employed to get rid of unwanted interference patterns caused by the high coherence.

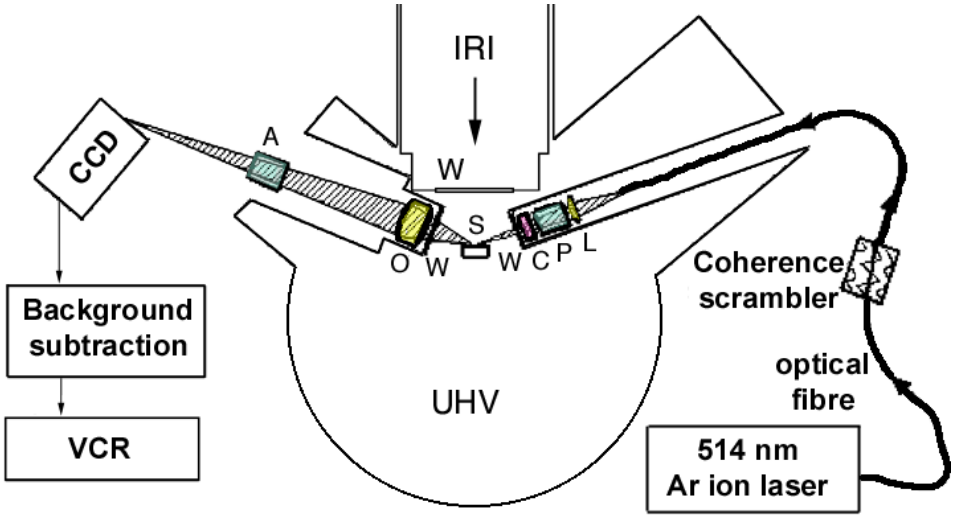

Fig. 2.4 Schematic view of the EMSI principal components: **L**ens, **P**olariser, **C**ompensator (λ/4 plate), **W**indow, **S**ample, **O**bjective lens, **A**nalyzer (polarizer).

An analyzer (a Glan-Thompson prism, like the polarizer) is fine-tuned to filter out the polarized light and obtain a *blank* image. If at this point some adsorbate is deposited on the surface, then the optical properties are locally changed and some intensity appears in the EMSI image, as detected by a CCD camera, which is tilted to partially correct the ineluctable distortion of the EMSI images. To maximize the contrast, an Argus 20 (Hamamatsu) unit performs a real-time background subtraction. Compared to PEEM, EMSI has a 10 times lower spatial resolution, but, the big advantage of being applicable at any pressure [4].

2.3 Infrared Thermography – IRT

For precise spatially resolved temperature measurements an IR (Radiance PM-Lab, Amber) camera with a spectral range of 3–5 µm and a lateral resolution of about 20 µm has been used. The radiation is collected by a 256 x 256 InSb array detector cooled at 77 K. The setup includes a MgF_2 window and a 100 mm Ge objective. Despite the high quality of the IR-camera, the very low (0.02) emissivity of the Pt(110) surface compels meticulous experimental attention.

2.4 The sample

For the experiment described in Chapter 3, a platinum crystal with a diameter of 10 mm and thickness of 1.5 mm, cut in the [110] direction and polished at the Crystal Lab of the FHI was prepared. It was then mounted on a 5-degree-of-freedom sample holder inside the vacuum chamber, where the crystal, normally grounded, can be heated (by a 250 W Osram Xenophot HLX halogen lamp) and cooled (by a LN line). The temperature is monitored using a K-Type chromel alumel thermocouple. The surface is prepared by heating in an oxygen atmosphere ($1\cdot 10^{-6}$ mbar) and repeated cycles of Ar ions sputtering at 500 K and annealing at 1400 K, until a clear LEED pattern is observed. The thin samples employed in the SAW and laser experiments are described later in Chapter 6.

[1] W. Engel, M. E. Kordesch, H. H. Rotermund, S. Kubala, and A. v. Oertzen, *A UHV-compatible photoelectron emission microscope for applications in surface science*, Ultramicroscopy **36**, 148 (1991).

[2] R. H. Fowler, *The analysis of photoelectric sensitivity curves for clean metals at various temperatures*, Phys. Rev. **38**, 45 (1931).

[3] D. Beaglehole, *Performance of a microscopic imaging ellipsometer*, Rev. Sci. Instrum. **59**, 2557 (1988).

[4] H. H. Rotermund, G. Haas, R. U. Franz, R. M. Tromp, and G. Ertl, *Imaging pattern formation in surface reactions from ultra-high vacuum to atmospheric pressures*, Science **270**, 608 (1995).